Science Advances
AAAS

Supplementary Materials for

Activation mechanism of a short argonaute-TIR prokaryotic immune system

Dongchun Ni *et al.*

Corresponding author: Henning Stahlberg, henning.stahlberg@epfl.ch;
Babatunde Ekundayo, babatunde.ekundayo@epfl.ch; Dongchun Ni, dongchun.ni@epfl.ch

Sci. Adv. **9**, eadh9002 (2023)
DOI: 10.1126/sciadv.adh9002

The PDF file includes:

Other Supplementary Material for this manuscript includes the following:

Materials and Methods

Plasmid constructs design and cloning

To reconstitute the *M. polysiphoniae* SPARTA complex, *M. polysiphoniae* pAgo was co-expressed with *M. polysiphoniae* TIR-APAZ using two plasmids. Full-length *M. polysiphoniae* pAgo codon-optimized for *E. coli* was synthesized with a sequence for an N-terminal Tobacco Etch Virus (TEV) cleavage site and cloned (GenScript Biotech) into pMAL-c4x plasmid to be in-frame with an N-terminal Maltose Binding protein (MBP) tag. Full-length *M. polysiphoniae* TIR-APAZ codon-optimized for *E. coli* was synthesized with a sequence for a N-terminal 6xHis tag and TEV cleavage site and cloned (GenScript Biotech) into pET24a plasmid. In this way, both genes were inserted downstream of a LacI repressed T7 promoter to facilitate inducible expression using Isopropyl β-D-1-thiogalactopyranoside (IPTG).

Protein expression and purification

The *M. polysiphoniae* SPARTA complex composed of *Map*Ago and *Map*TIR-APAZ were coexpressed and purified from *E. coli* BL21(DE3) Star. For expression, chemically competent *E. coli* BL21(DE3) Star was transformed with both, the pMAL-c4x plasmid containing the ampicillin resistance gene for expression of *Map*Ago and the pET24a plasmid containing kanamycin resistance gene for the expression of *Map*TIR-APAZ, and grown overnight at 37°C on LB-agar plates containing both selection antibiotics (50 μg/mL kanamycin and 100 μg/mL carbenicillin). The colonies obtained were transferred to 100 mL of 2xYT media containing selection antibiotics and grown overnight at 37°C with shaking. 60ml of the overnight culture was used to inoculate 6L of 2xYT media containing selection antibiotics. The cultures were grown until they reached an absorbance at 600nm of 0.5-0.7, then incubated at 4°C for 1 hour, before inducing protein expression with 0.5mM Isopropyl

β-D-1-thiogalactopyranoside (IPTG) for 18 hours at 20°C. The cultures were harvested by centrifugation at 3,000 xg for 30 mins at 4°C. The resulting supernatant was discarded, and the pellet was resuspended in 100 mL of precooled lysis buffer (25 mM HEPES-NaOH, pH 7.5, 500 mM NaCl, 10% glycerol, 25 mM imidazole, 1mM β-mercaptoethanol) supplemented with 2 tablets of cOmplete™ EDTA-free Protease Inhibitor Cocktail (Roche) before lysis by sonication. The lysate was clarified by centrifugation for 30 min at 70,560 × *g* at 4°C in an Optima XPN Ultracentrifuge (Beckman Coulter) using a Ti-45 rotor. The supernatant, which contained soluble 6xHis-tagged *Map*TIR-APAZ in complex with MBP tagged *Map*Ago, was loaded onto 5 mL of HisPur™ Ni-NTA Resin (Thermo Scientific) pre-equilibrated with wash buffer (25 mM HEPES-NaOH, pH 7.5, 500 mM NaCl, 10% glycerol, 25 mM imidazole, 1mM β-mercaptoethanol) in an XK16/20 column (Cytiva Life Sciences). After loading, the column was washed with 50 mL of wash buffer and eluted with 10 mL elution buffer (25 mM HEPES-NaOH, pH 7.5, 500 mM NaCl, 10% glycerol, 400 mM imidazole, 1mM β-mercaptoethanol). Pooled elution fractions were loaded onto 3ml of amylose resin (New England Biolabs) pre-equilibrated with amylose wash buffer (25mM HEPES pH7.5, 200mM NaCl, 10% glycerol, 1mM DTT). Upon complete loading, the column was washed with amylose wash buffer and eluted with 10ml of amylose elution buffer (25mM HEPES pH7.5, 200mM NaCl, 10% glycerol, 1mM DTT, 20mM maltose). The pooled elution fraction was concentrated to ∼500 µl in 50 K Amicon Ultra-15 concentrators (Millipore, Billerica, MA) and further purified by gel filtration chromatography on a 10/300 GL Superdex 200 gel filtration column (Cytiva Life Sciences) in gel filtration buffer (25 mM HEPES-NaOH pH7.5, 150 mM NaCl, 10% glycerol and 1 mM DTT). Peak fractions as determined by the chromatograms at UV 280 generated from the Unicorn software (version 7.1) containing complete SPARTA complexes of subunits *Map*Ago and *Map*TIR-APAZ as determined by SDS-PAGE analysis were pooled, concentrated, flash frozen, and stored at −80°C.

For the reconstitution of guide RNA-bound SPARTA complex, 2 μM of purified SPARTA was mixed with 2 μM guide-RNA in reconstitution buffer (25 mM HEPES-NaOH pH7.5, 125 mM NaCl, 3 mM MgCl2, and 1 mM DTT) and incubated at 37°C for 15mins. After incubation the sample was loaded onto 10/300 GL Superdex 200 gel filtration column (Cytiva Life Sciences) in gel filtration buffer (25 mM HEPES-NaOH pH7.5, 125 mM NaCl, 3 mM MgCl2 and 1 mM DTT). The sample was concentrated to an A280nm of 0.8 using a 50 K Amicon Ultra-15 concentrator (Millipore, Billerica, MA) and was ready for cryo-EM experiments. For the reconstitution of heteroduplex-bound SPARTA complex after incubation with guide-RNA as previously described, the sample was further incubated with target-DNA for 30mins at 37°C. Following incubation, the sample was loaded onto 10/300 GL Superose 6 gel filtration column (Cytiva Life Sciences) in gel filtration buffer (25 mM HEPES-NaOH pH7.5, 125 mM NaCl, 2 mM MgCl2 and 1 mM DTT), gel filtration peaks corresponding to heteroduplex-bound SPARTA tetramers and monomers were separately concentrated to an absorption at 280 nm (A280nm) of 0.8 in 50 K Amicon Ultra-15 concentrators (Millipore, Billerica, MA) and were ready to be used for cryo-EM experiments. Samples not used for cryo-EM were mixed with an equal volume of buffer containing 25 mM HEPES-NaOH pH7.5, 200 mM NaCl, 20% glycerol and 1 mM DTT and were flash frozen for storage at −80°C.

SDS-PAGE Analysis

To evaluate the purity of the SPARTA complex and the presence of the individual pAgo and TIR-APAZ subunits in the complex, an SDS-PAGE analysis was performed. 20 μL of protein sample was supplemented with 5 μL of 4X NuPAGE LDS Sample Buffer (Thermo Scientific). Samples were incubated at 95°C for 10 minutes before loading on 4-12% SurePAGE™ Bis-Tris precast gels (Witec AG). Spectra™ Multicolor broad range protein

ladder (10 to 180 kDa) was also loaded on the gel to run as a size marker. Gels were run in 1x Tris-MOPS SDS running buffer (Witec AG) at 200 V for 30 minutes, washed briefly in MilliQ water and stained for 2 hours with QuickBlue Protein Stain (LuBioScience GmbH) with shaking. Gels were washed in MilliQ water before imaging on an iBright FL1500 Imaging System (Thermo Scientific).

Urea-PAGE analysis

To evaluate the presence of bound nucleic acids in the ssRNA or heteroduplex bound SPARTA complex, Urea-PAGE analysis was performed on peak fractions from the gel filtration of the complexes. Following gel filtration, samples from the peak fraction were incubated with Urea and Proteinase K (Thermo Fisher Scientific) at final concentrations of 0.1 M and 1 µg/µL, respectively and incubated at 50°C for 15 minutes. 2x loading dye (1 x TBE, 12% Ficoll, 7M Urea) was added to the reaction to a final 1x concentration, followed by heating at 95°C for 5 minutes before loading on a 15% Novex PAGE Tris-borate-EDTA (TBE)-Urea gel (Thermo Fisher Scientific). For nuclease digestion, 20ul of heteroduplex bound MapSPARTA with absorption at 280 nm (A280nm) of 0.8 was digested with excess amounts of RNAseA (Thermo Fisher Scientific), Micrococcal nuclease (Mnase) (New England Biolabs), RNaseIII (New England Biolabs) and DNaseI (Sigma-Aldrich) for 1 hour at 37 °C before proteinase K treatment and gel loading. The gel was run at 200V for 45 minutes and stained with 1x GelRed® Nucleic Acid Gel Stain for 30 minutes before imaging on an iBright FL1500 Imaging System (Thermo Fisher Scientific).

NAD/NADH quantification

SPARTA samples at a concentration of 0.5 µM were incubated with 10 µM of NADH for 2 hours at 37°C. 50 µL of each sample was used as input for the NAD/NADH Quantitation Kit

(Sigma-Aldrich, MAK037-1KT) according to the instructions provided by the manufacturer. The measurements were repeated in at least triplicates to obtain statistically significant results.

Mass photometry

Mass Photometry experiments were carried out using a Refeyn TwoMP (Refeyn Ltd., Oxford, UK) MP system. AcquireMP and DiscoverMP software packages were used to record movies and analyse data, respectively using standard settings. Microscope coverslips (high precision glass coverslips, Marienfeld) were cleaned following the Refeyn Ltd Indvidual rinsing procedure. Reusable self-adhesive silicone culture wells (Grace Bio-Labs reusable CultureWell™ gaskets) were used to keep the sample droplet shape. Contrast-to-mass calibration was carried out using BSA (Albumin, Bovine Serum Fraction V, low heavy metals, Millipore), giving molecular weights of 66, 132, 198, 264 kDa. Immediately before the measurements, protein stocks were diluted directly in a buffer containing 25 mM HEPES-NaOH pH7.5, 125 mM NaCl, 2 mM MgCl2. To this end, 1 to 2 µL of protein solution was added into 18 to 19 µL of analysis buffer to reach a final drop volume of 20 µL.

Cryo-EM sample preparation and data collection

Cryo-EM grids for apo SPARTA monomer, guide-RNA-bound SPARTA monomer, heteroduplex-bound SPARTA monomer, heteroduplex-bound SPARTA tetramer was prepared by applying 3 µl of concentrated sample onto 400-mesh R1.2/1.3 UltrAuFoil grids (Quantifoil Micro Tools GmbH), which were rendered hydrophilic by glow discharging at 15 mA for 90 seconds with a PELCO easiGlow device (Ted Pella, Inc.). The sample was adsorbed for 30 sec on the grids, followed by blotting and plunge freezing into liquid ethane using a Vitrobot Mark IV plunge freezer (Thermo Fisher Scientific). For the heteroduplex-bound SPARTA tetramer supplemented with NAD, after application of 3 µl of the

concentrated sample on the grid, 0.5 µl of 50mM beta-Nicotinamide adenine dinucleotide sodium salt (Sigma Aldrich GmbH) was added directly to the sample followed by immediate plunge freezing. Cryo-EM data were collected using the automated data acquisition software EPU (Thermo Fisher Scientific) on a Titan Krios G4 transmission electron microscope (Thermo Fisher Scientific), operating at 300kV and equipped with a cold-FEG electron source and a Falcon4 direct detection camera. Images were recorded in counting mode at a nominal magnification of 96kx, corresponding to a physical pixel size of 0.726 Å and 0.5082 Å at the sample level. Datasets were collected at a defocus range of 0.8 to 2.5 µm with a total electron dose of 60 $e^-/Å^2$. Image data were saved as Electron Event Recordings (EER).

Cryo-EM image processing, model building, and refinement

The cryo-EM image processing was performed using cryoSPARC v3.4 (29).

The EM movie stacks were aligned and dose weighted using the patch-based motion correction (cryoSPARC implementation). CTF estimation was performed using the patch-based option as well. For the data of apo SPARTA monomer, blob picker was used for initial particle picking, which resulted in 200,000 particles from the initial 1000 images. These particles were used for two rounds of 2D classification to generate templates for template-based particles picking on the full dataset, resulting in 2,821,100 particles. Multiple rounds of 2D classifications were performed and junk particles were deselected. Ab-initio reconstruction and hetero-refinement yielded multiple 3D classes. The best 3D class consisting of 85,650 particles used for non-uniform refinement yielded a cryo-EM map at 3.74 Å overall resolution in C1 symmetry **(Fig. S4)**.

The 2D classes generated from apo SPARTA monomer were used for template picking for the guide RNA-bound SPARTA monomer datasets. This resulted in 1,941,707 particles. Several rounds of 2D classification, ab-initio reconstruction and hetero-refinement resulted in

a map at 7.11 Å overall resolution in C1 symmetry from 59,152 particles **(Fig. S5)**. The SPARTA tetramer samples were processed using the blob picker for particle picking, 2D classification, template generation and template picking. Multiple rounds of 3D classification and hetero-refinement resulted in three distinct states of the SPARTA dimer at an overall resolution of 3.3 - 3.9 Å overall resolution in C2 symmetry. Dimer states 1, 2 and 3 consisted of 59,663, 36,541 and 25,123 particles, respectively **(Fig. S2)**. The duplex-bound monomer was also resolved from 44,404 particles at 4.8 Å overall resolution **(Fig. S2)**. The apo SPARTA tetramer could also be resolved to 3.9 Å from 14,276 particles using a similar processing strategy **(Fig. S4)**. The NAD-supplemented tetramer was also processed with a similar approach. 3D classification resulted in three structures which contained three distinct ligand conformations. These three states were referred to as the pre-hydrolyzed, hydrolysed, and pre-released states. Each state contained 65,473, 50,287 and 52,117 particles respectively at an overall resolution of 3.2 - 3.7 Å overall in C1 symmetry **(Fig. S2)**.

Atomic models for all nine were mostly manually built *de novo* in Coot 0.9.4 (*30*). For low-resolution or low-quality regions, an AlphaFold2 (ColabFold implementation) prediction was used as a guide for amino acid assignment and backbone tracing (*31*). Real-space refinement for all built models was performed using Phenix, version 1.19.2-4158 by applying a general restraints setup (*32*).

Data visualization

Structural alignments and superpositions were performed with PyMOL (The PyMOL Molecular Graphics System, Version 1.8.2.0 Schrödinger, LLC) and UCSF ChimeraX v 1.4. Gel images were processed and prepared on ImageJ (Version 1.53k). Figures were rendered using PyMOL, UCSF Chimera, ChimeraX (*33*), and Adobe Illustrator (https://adobe.com/products/illustrator).

References

29. A. Punjani, J. L. Rubinstein, D. J. Fleet, M. A. Brubaker, cryoSPARC: algorithms for rapid unsupervised cryo-EM structure determination. *Nat. Methods*. **14**, 290–296 (2017).

30. P. Emsley, B. Lohkamp, W. G. Scott, K. Cowtan, Features and development of Coot. *Acta Crystallogr. D Biol. Crystallogr.* **66**, 486–501 (2010).

31. J. Jumper, R. Evans, A. Pritzel, T. Green, M. Figurnov, O. Ronneberger, K. Tunyasuvunakool, R. Bates, A. Žídek, A. Potapenko, A. Bridgland, C. Meyer, S. A. A. Kohl, A. J. Ballard, A. Cowie, B. Romera-Paredes, S. Nikolov, R. Jain, J. Adler, T. Back, S. Petersen, D. Reiman, E. Clancy, M. Zielinski, M. Steinegger, M. Pacholska, T. Berghammer, S. Bodenstein, D. Silver, O. Vinyals, A. W. Senior, K. Kavukcuoglu, P. Kohli, D. Hassabis, Highly accurate protein structure prediction with AlphaFold. *Nature*. **596**, 583–589 (2021).

32. D. Liebschner, P. V. Afonine, M. L. Baker, G. Bunkóczi, V. B. Chen, T. I. Croll, B. Hintze, L. W. Hung, S. Jain, A. J. McCoy, N. W. Moriarty, R. D. Oeffner, B. K. Poon, M. G. Prisant, R. J. Read, J. S. Richardson, D. C. Richardson, M. D. Sammito, O. V. Sobolev, D. H. Stockwell, T. C. Terwilliger, A. G. Urzhumtsev, L. L. Videau, C. J. Williams, P. D. Adams, Macromolecular structure determination using X-rays, neutrons and electrons: recent developments in Phenix. *Acta Crystallogr D Struct Biol*. **75**, 861–877 (2019).

33. T. D. Goddard, C. C. Huang, E. C. Meng, E. F. Pettersen, G. S. Couch, J. H. Morris, T. E. Ferrin, UCSF ChimeraX: Meeting modern challenges in visualization and analysis. *Protein Sci.* **27**, 14–25 (2018).

Supplementary Figures

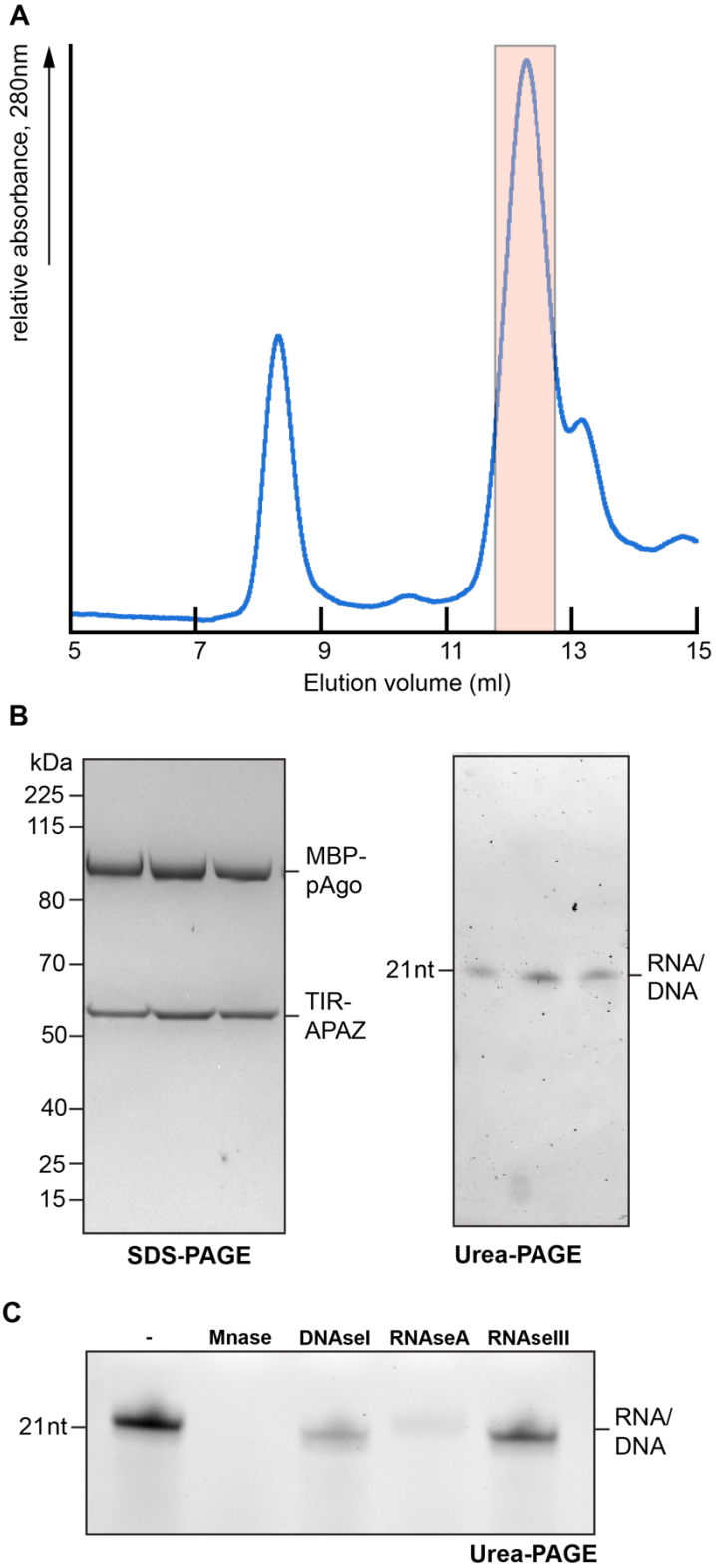

Fig. S1. Purification of the MapSPARTA complex. (A) Superdex 200 gel filtration chromatogram at absorbance of 280 nm for purified MapSPARTA complex. Red box indicated the peak fraction containing complexes of pAgo and TIR-APAZ. (B) SDS-PAGE gel of the purified MapSPARTA complex on the left panel and Urea-PAGE gel showing the bound heteroduplex and its treatment with different nucleases in (C).

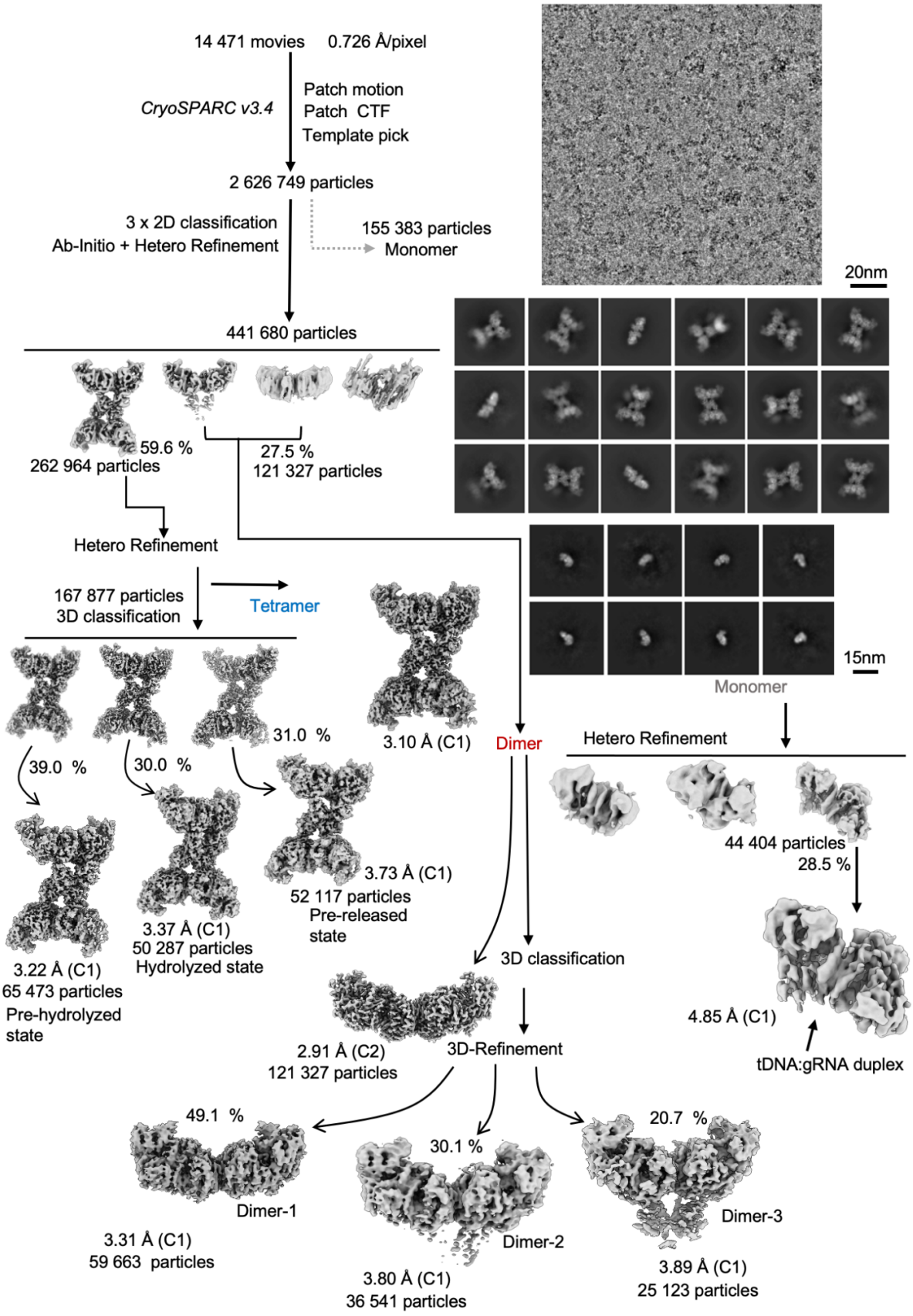

Fig S2: Cryo-EM data processing workflow for MapSPARTA tetramer with NAD

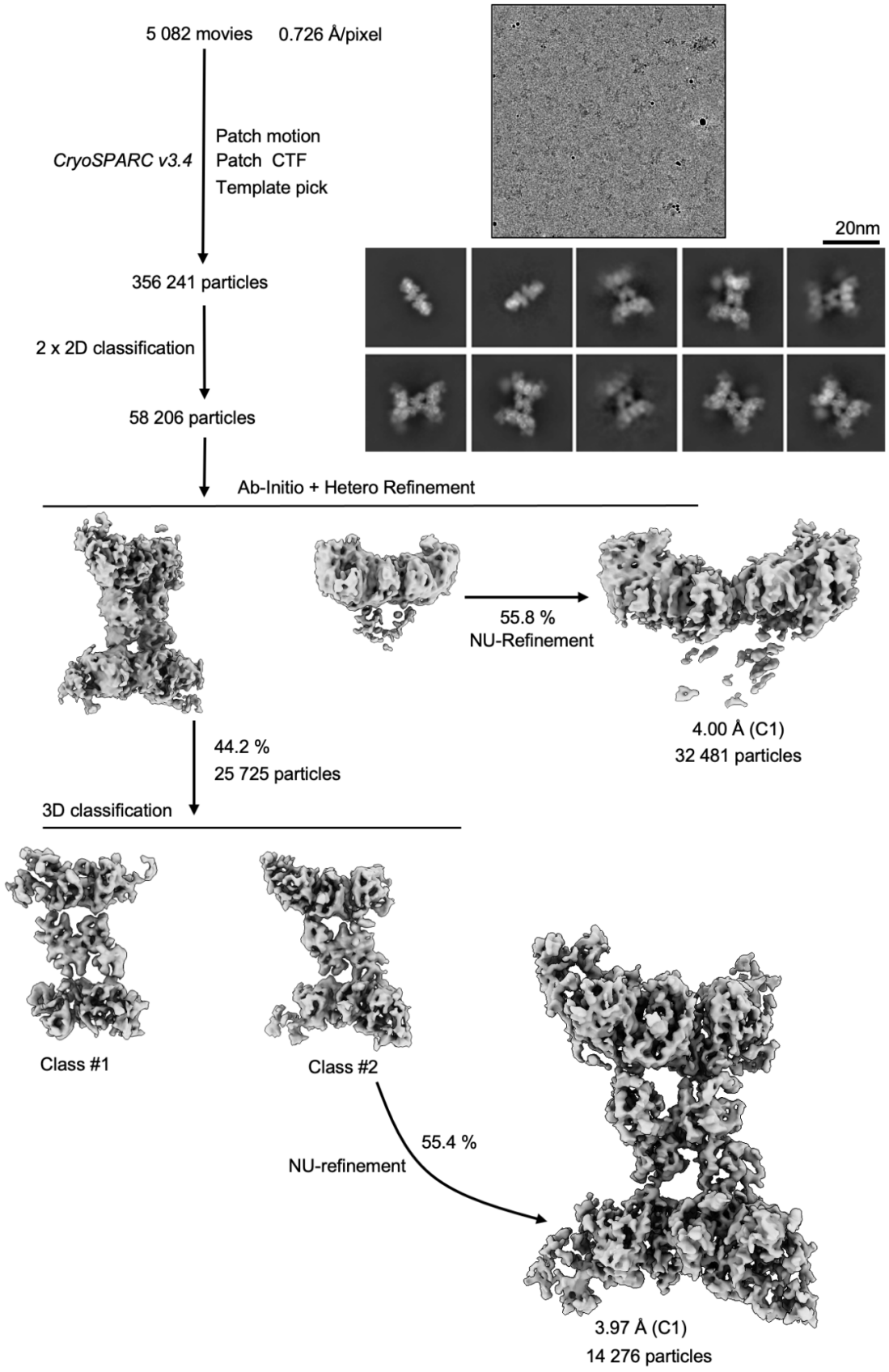

Fig S3: Cryo-EM data processing workflow for MapSPARTA tetramer without NAD

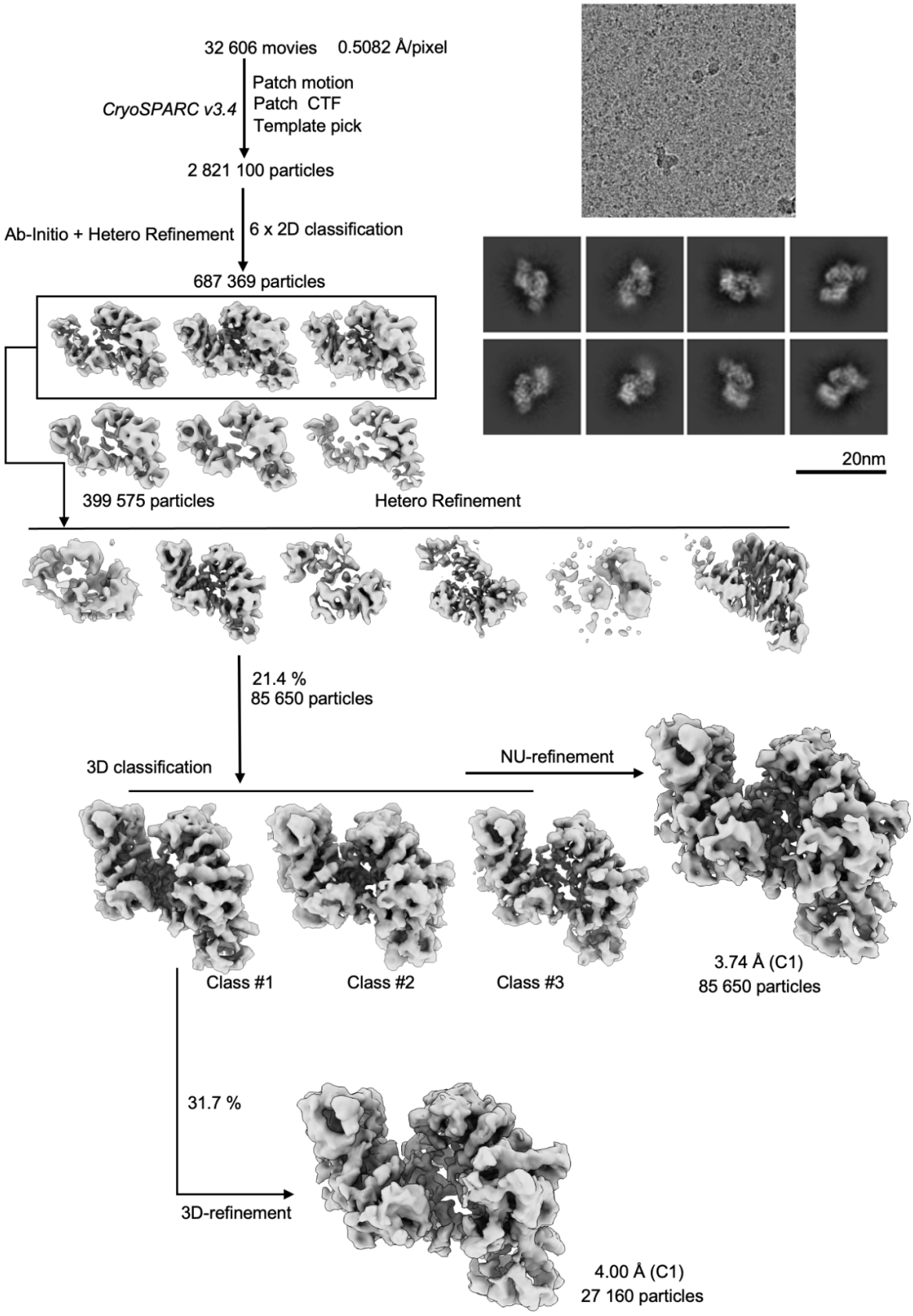

Fig S4: Cryo-EM data processing workflow for apo form MapSPARTA monomer

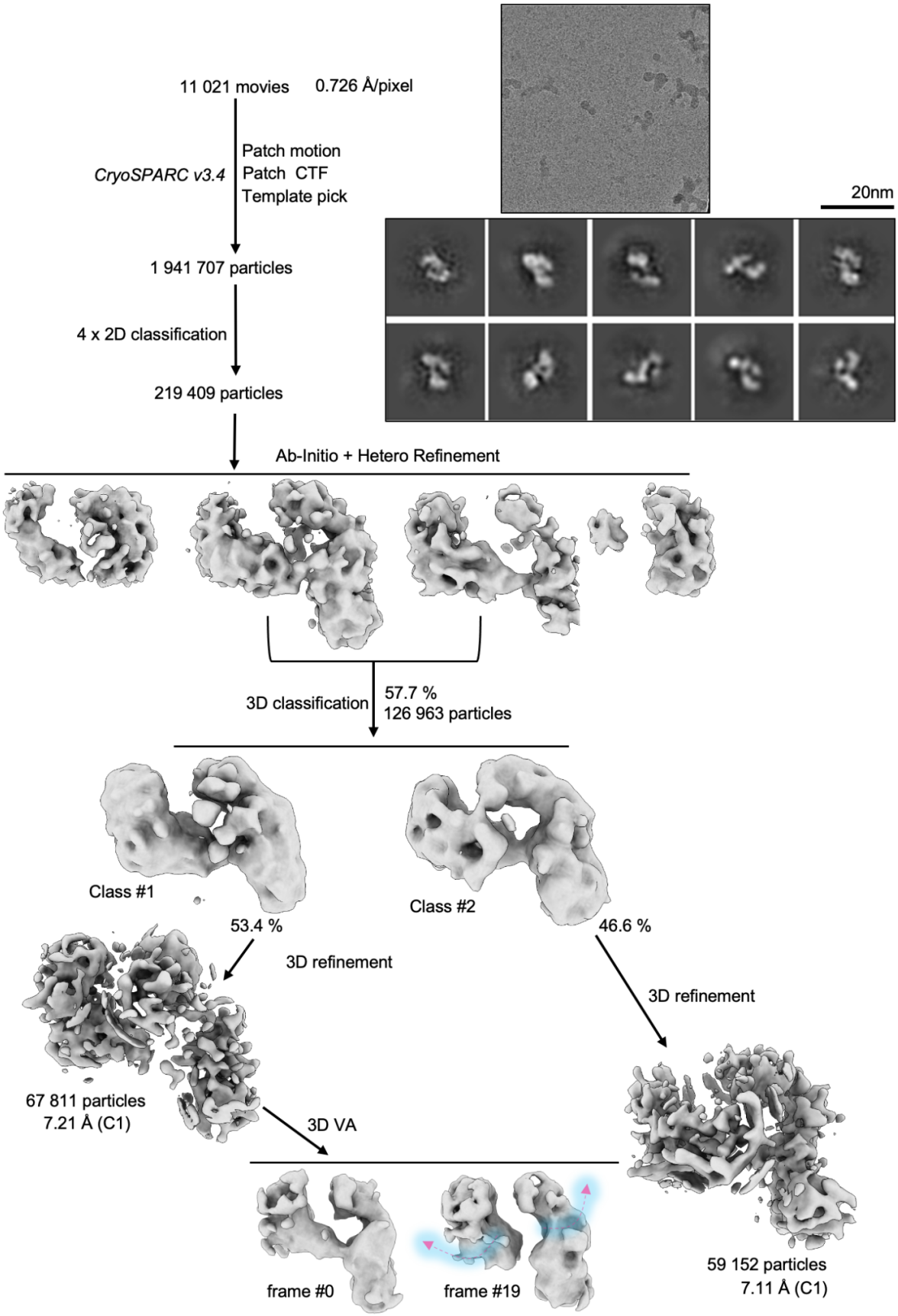

Fig S5: Cryo-EM data processing workflow for MapSPARTA monomer bound to guide-RNA

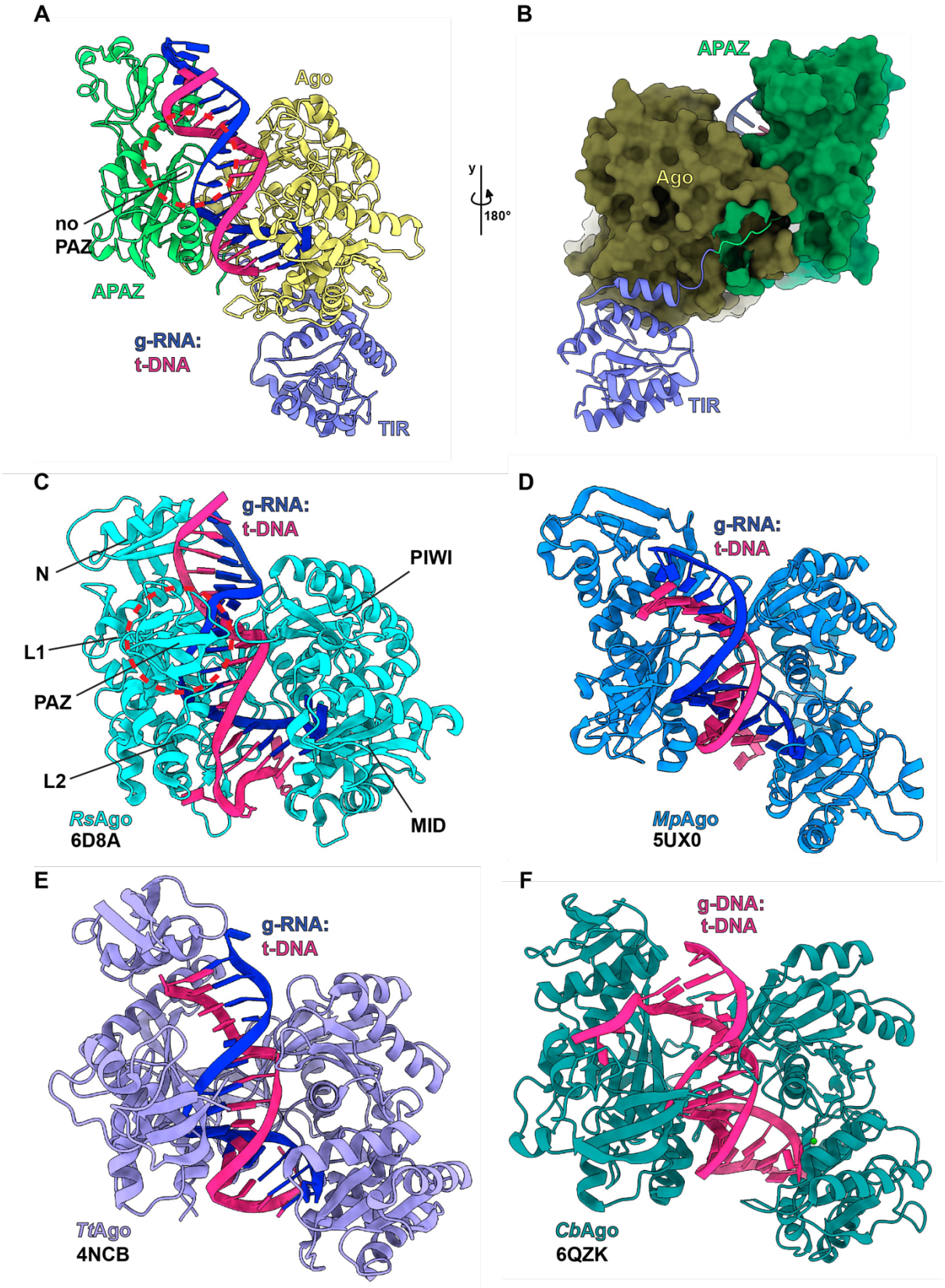

Fig. S6. Structure comparison of pAgos with the Ago module of MapSPARTA. (A and B) Cartoon and surface representations of heteroduplex-bound MapSPARTA revealing Ago and APAZ constitute the Ago module. Red circle indicates the position of PAZ domain. (C-F) Structures of duplex bound pAgos (*4*, *17–20*).

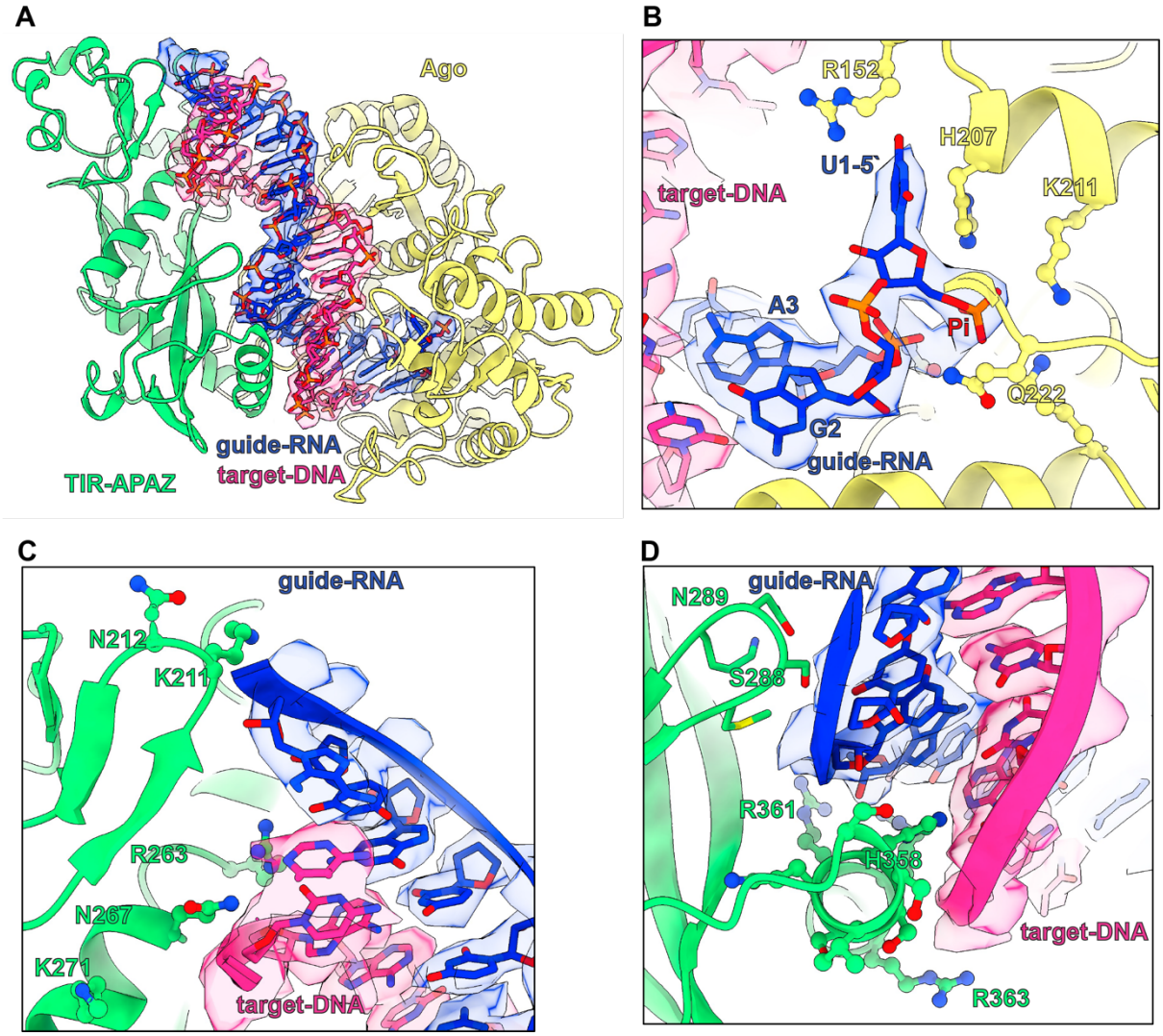

Fig. S7. Details of nucleic acid interactions with the Ago module of MapSPARTA. (A) Cartoon representation of heteroduplex-bound MapSPARTA with the cryo-EM density around the bound duplex. (B) Details of the interactions between the 5`-phosphate and U1 nucleotide of guide-RNA with residues from Ago. (C) Details of the interactions between the 3` guide-RNA and 5` target-DNA with residues from APAZ. (D) Details of the interactions between the heteroduplex of the major groove with residues from APAZ.

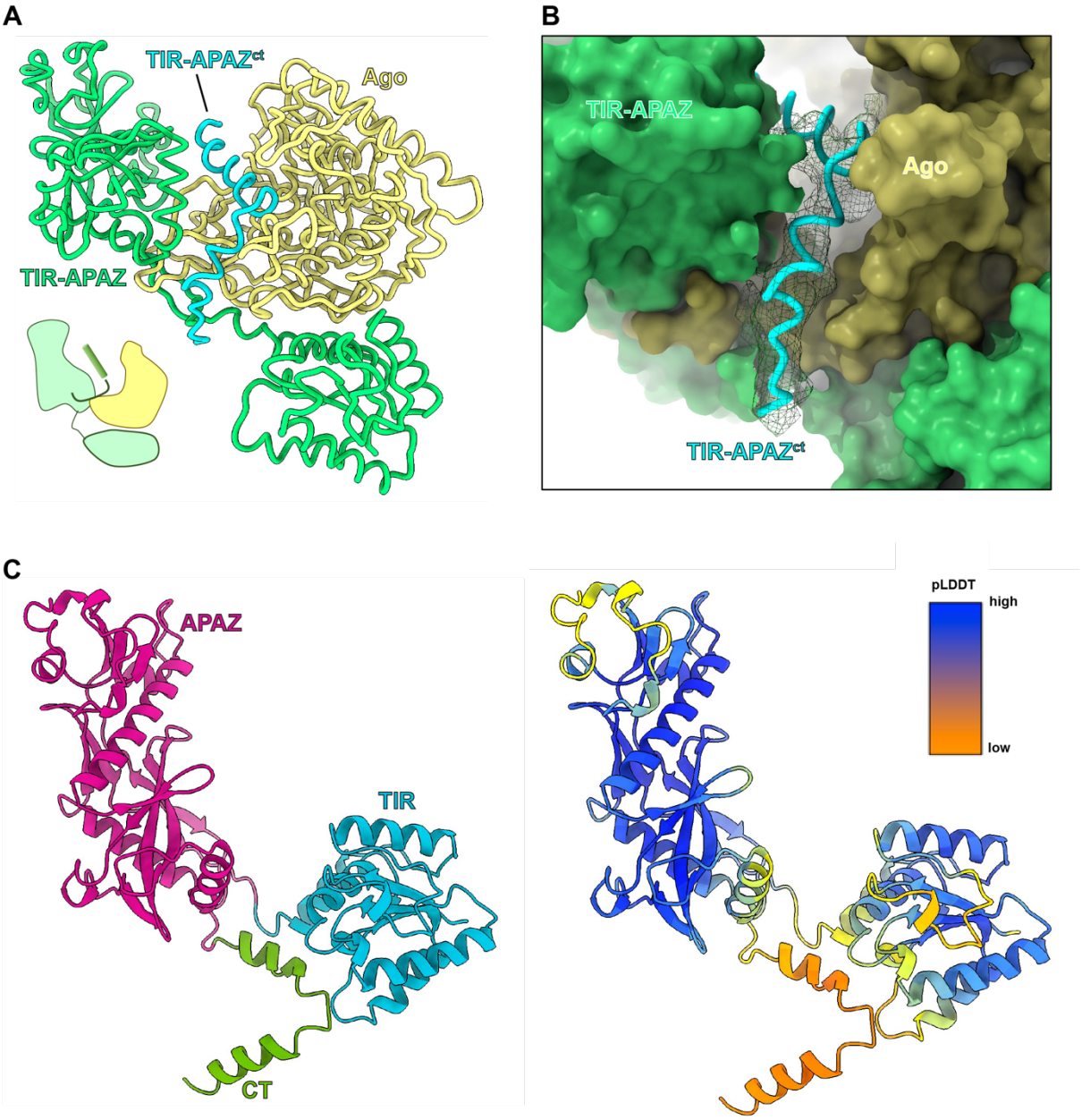

Fig. S8. Structure of the apo form MapSPARTA. (A) Cartoon representation of apo form MapSPARTA with the inhibitory helix located between indicated. (B) Cryo-EM density of the inhibitory helix located between Ago and TIR-APAZ in surface representation (C) Alphafold2 model for the TIR-APAZ showing the low confidence prediction for the C-terminal inhibitory helix.

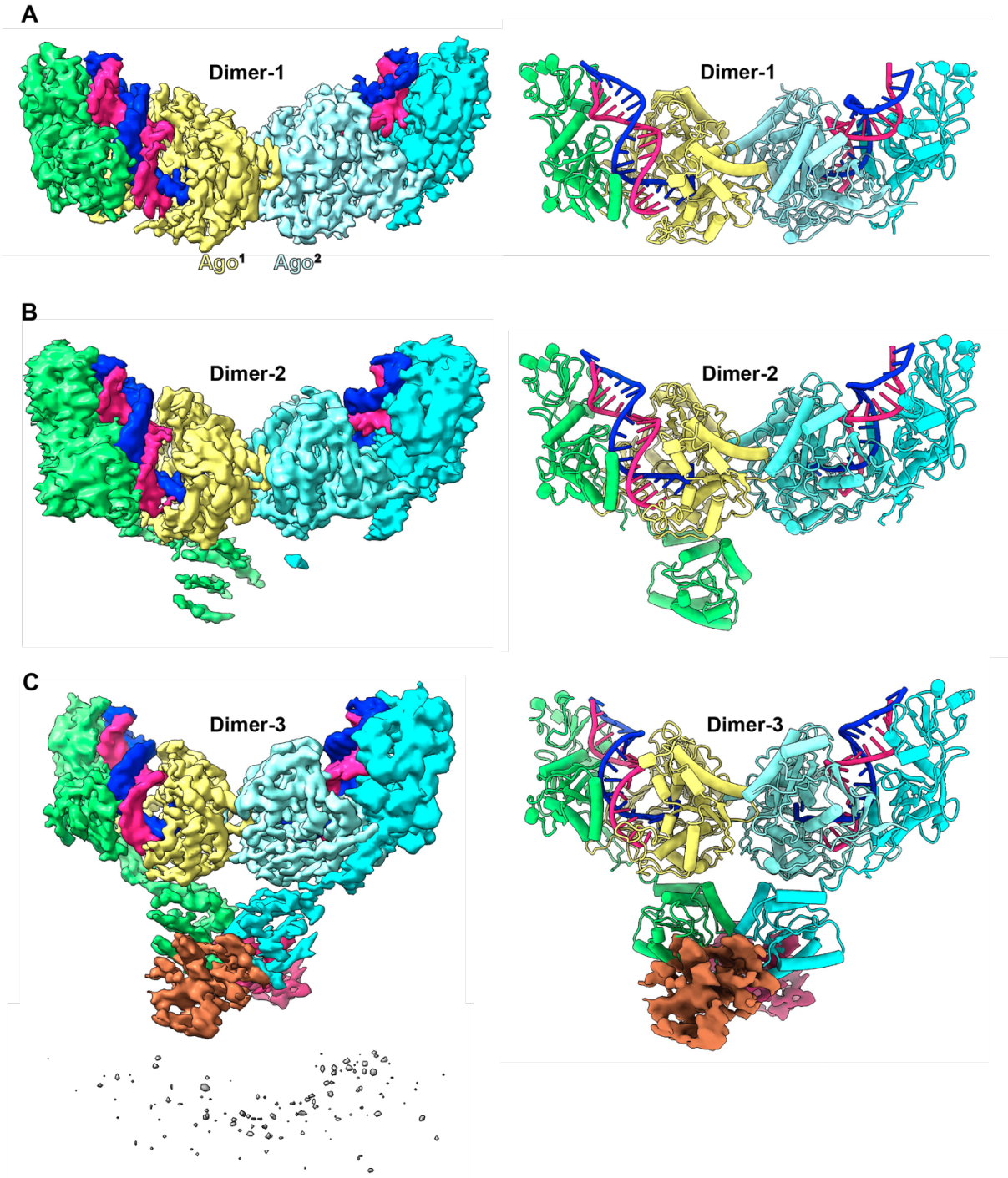

Fig. S9. Structure of MapSPARTA dimers. (A, B and C) Cryo-EM density maps and structures of MapSPARTA dimers in states 1, 2 and 3.

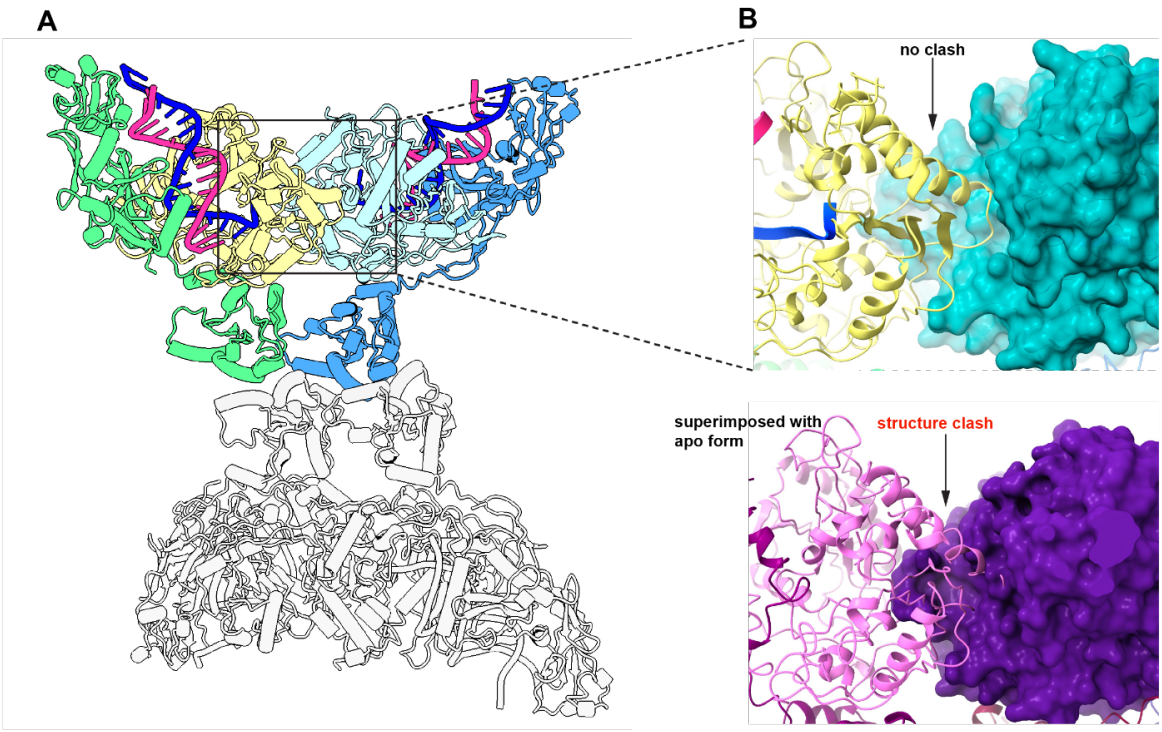

Fig. S10. MapSPARTA-pAgo dimerization interface . (A) Cartoon representation of a MapSPARTA tetramer with one of the pseudo-symmetric dimers in color. (B) Zoom-in of the dimerization interface of the pseudo-symmetric dimers showing a structure clash when the apo form is superimposed.

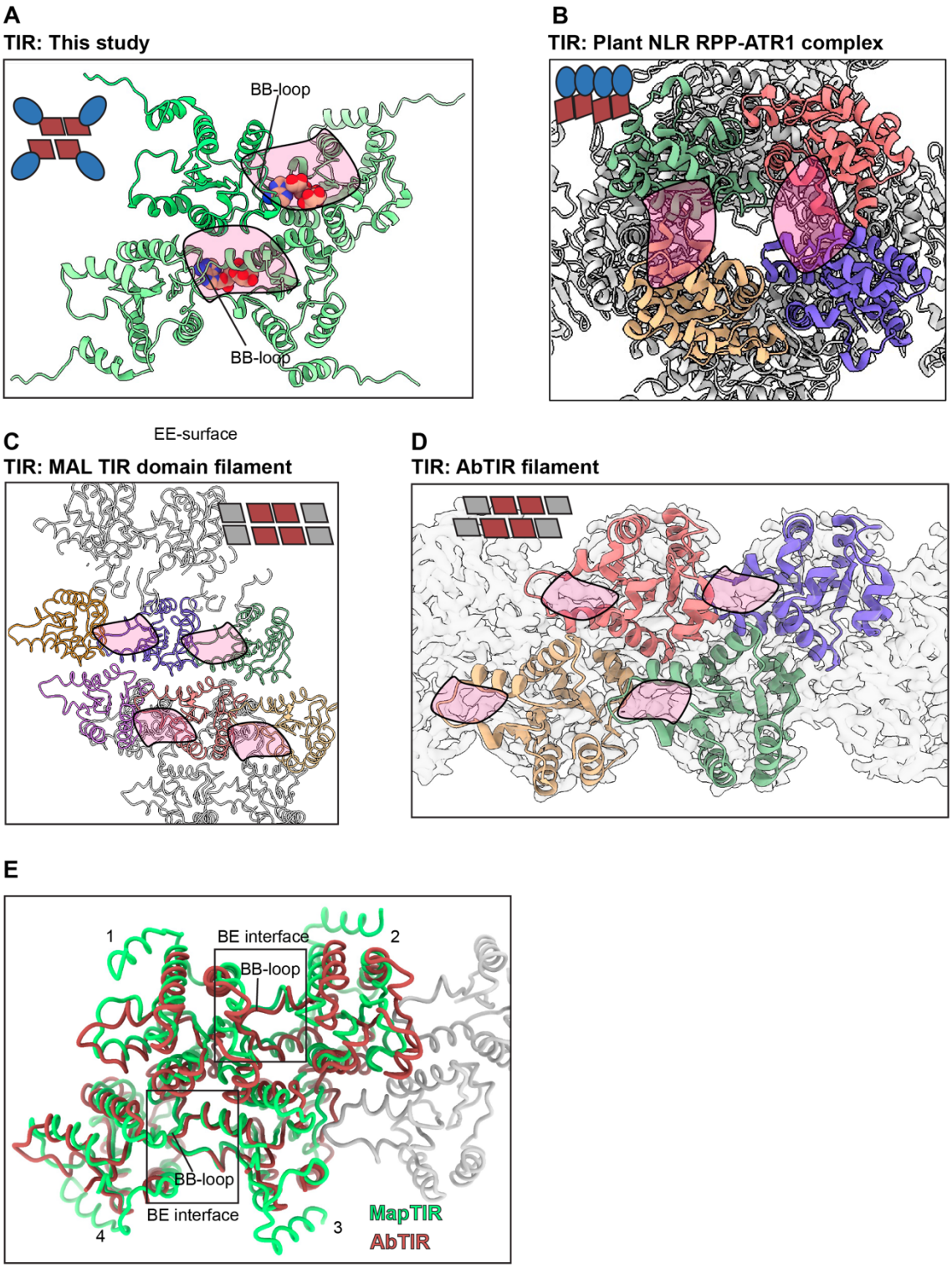

Fig. S11. Comparison of TIR assembly and catalytic sites . (A -D) Cartoon representations of the TIR arrangement from MapSPARTA tetramer from this study, Plant NLR TIR (pdb id: 7crc, 7jlx), MAL TIR (pdb id: 5uzb) and AbTir filament (pdb id: 7un8) (*21–23*). (E) Structure overlay between TIR tetramer from MapSPARTA and AbTir filament.

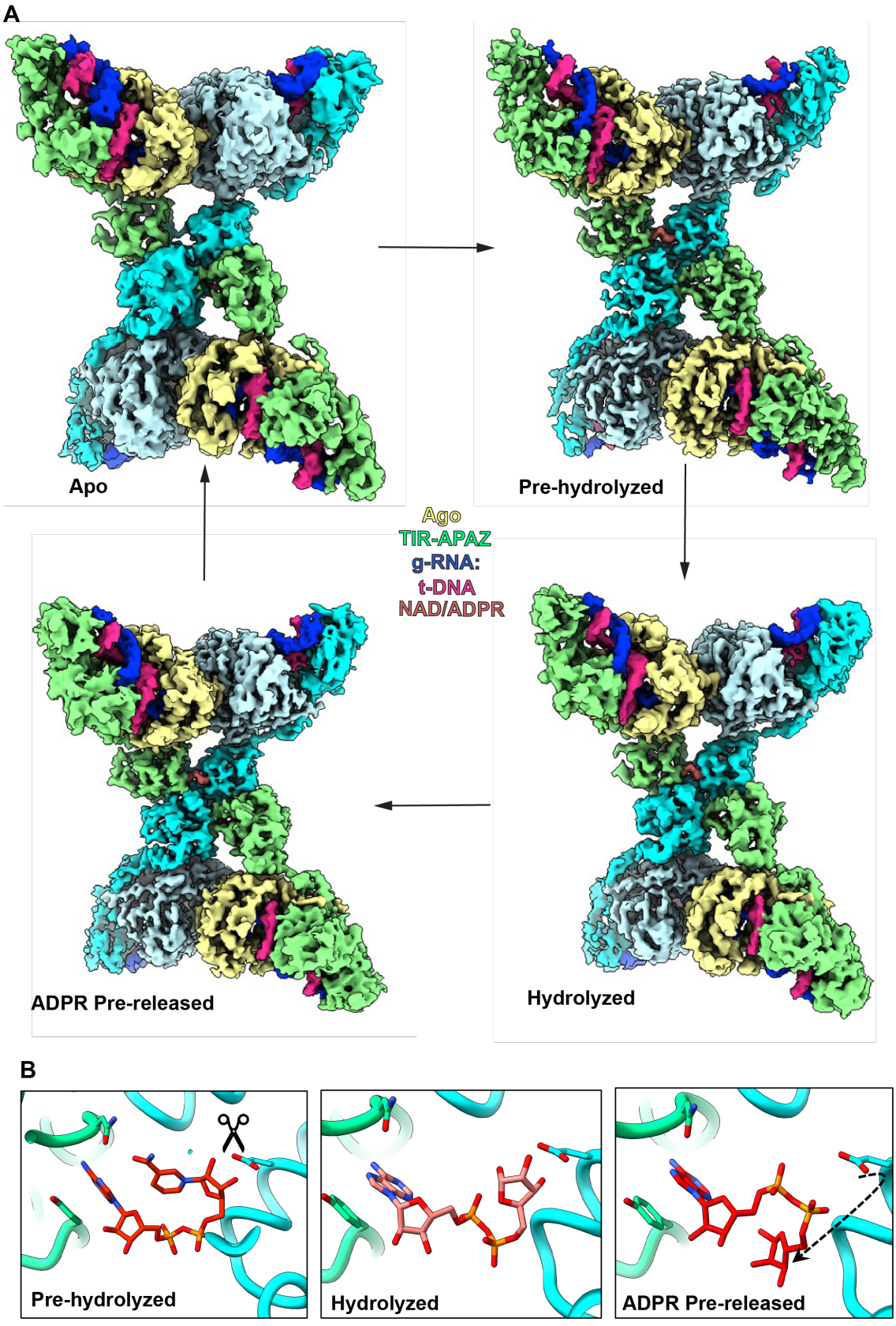

Fig. S12. Structures of MapSPARTA tetramer in different states of NADase action. (A) Cryo-EM density maps of MapSPARTA tetramer in apo, pre-hydrolysed, hydrolysed and pre-released states. (B) Structural changes from the NAD pre-hydrolysed to the ADPR pre-released states. Arrow in the third panel shows the flipping of the ribose moiety.

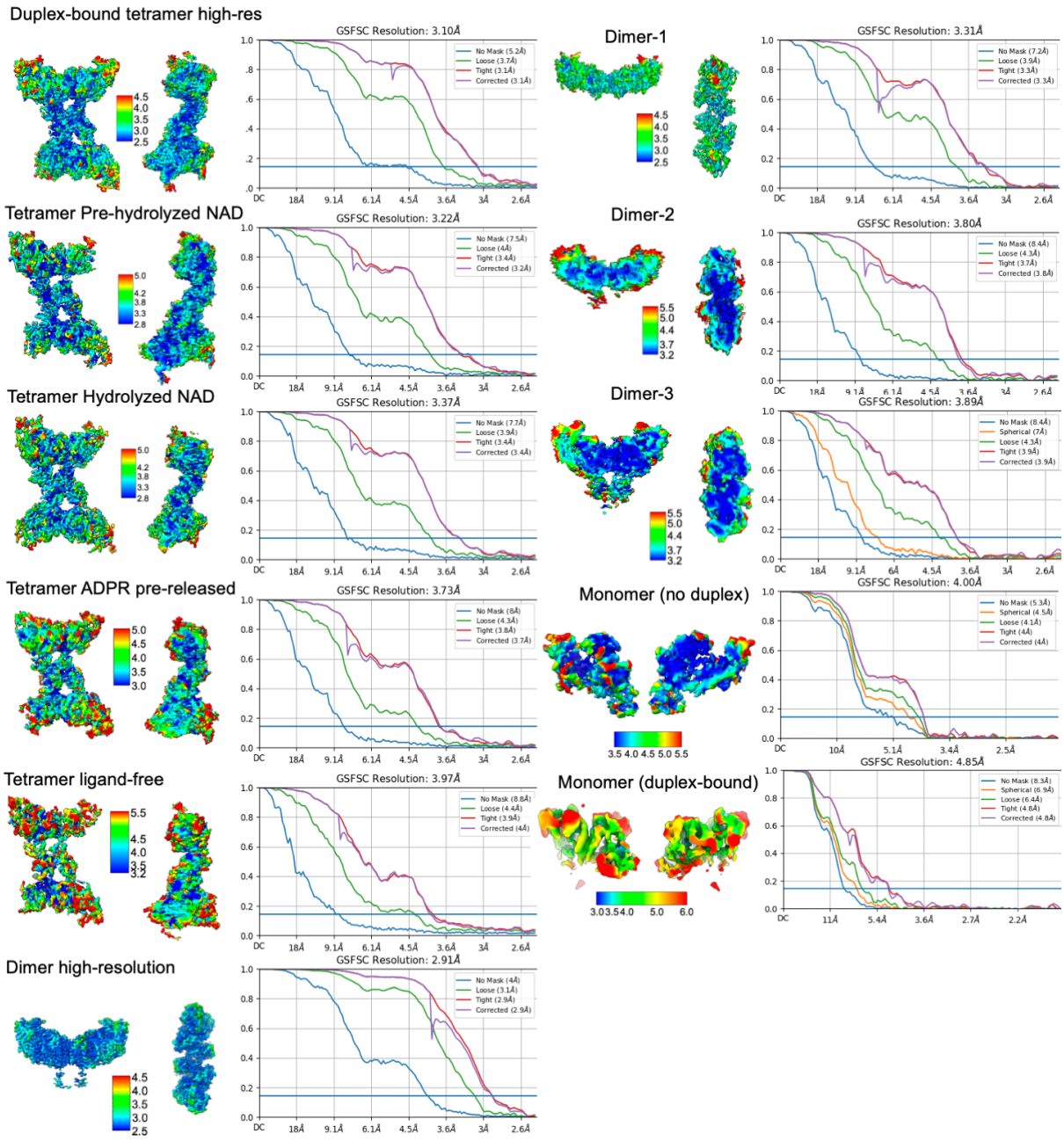

Fig S13: Fourier Shell Correlation (FSC) curves for cryo-EM maps generated in this study.

Table 1

	Tetramer ligand-free (EMD-17299) (PDB ID 8OZ6)	Duplex-bound tetramer high-resolution (EMD-17300)	Tetramer Pre-NAD cleavage (EMD-17310) (PDB ID 8OZI)	Tetramer Post-NAD cleavage-1 (EMD-17308) (PDB ID 8OZG)	Tetramer Post-NAD cleavage-2 (EMD-17307) (PDB ID 8OZF)	Dimer high-resolution (EMD-17306) (PDB ID 8OZE)	Dimer-1 (EMD-17301)	Dimer-2 (EMD-17302)	Dimer-3 (EMD-17305) (PDB ID 8OZD)	Monomer (duplex-bound) (EMD-17303)	Monomer (no duplex) (EMD-17304) (PDB ID 8OZC)
Data collection and processing											
Magnification	165kx	165kx									155kx
Voltage (kV)	300	300									300
Electron exposure (e–/Å^2)	50	60									60
Micrograph images	5 082	14 471									32 606
Defocus range (-μm)	0.8-2.5	0.8-2.5									0.8-2.0
Pixel size (Å)	0.726	0.726									0.5082
Symmetry imposed	C1	C1	C1	C1	C1	C2	C1	C1	C1	C1	C1
Initial particle images (no.)	356 241	2 626 749									2 821 100
		262 964				121 327				155 383	
Final particle images (no.)	14 276/25 725	167 877	65 473	50 287	52 117	121 327	59 663	36 541	25 123	44 404	27 160/85 650
Map resolution (Å)	3.97	3.10	3.22	3.37	3.73	2.91	3.31	3.80	3.89	4.85	4.00
FSC threshold	0.143	0.143	0.143	0.143	0.143	0.143	0.143	0.143	0.143	0.143	0.143
Map resolution range (Å)	30-3.1	30-2.5	30-2.6	30-2.9	30-3.0	30-2.4	30-2.5	30-3.1	30-3.2	30-3.5	30-3.2
Refinement											
Initial model used (PDB code)	n/a	n/a (de novo)	n/a	n/a	n/a	n/a (de novo)	n/a	n/a	n/a	n/a	n/a
Map sharpening B factor (Å2)	-20.0	-37.5	-25.6	-23.1	-12.8	-66.2	-46.4	-29.6	-36.6	-91.2	-109.2
Model composition											
Non-hydrogen atoms	32004	n/a	32092	32077	32076	13434	n/a	n/a	16002	n/a	7478
Protein residues	3564		3564	3564	3564	1448			1782		913
Nucleotide			136	136	136	74			68		0
Ligands			NAD:2	AR6:2	AR6:2						
R.m.s. deviations											
Bond lengths (Å)	0.005 (6)	n/a	0.004 (0)	0.003 (0)	0.003 (0)	0.003 (0)	n/a	n/a	0.003 (0)	n/a	0.002 (0)
Bond angles (°)	0.734 (37)		0.680 (31)	0.688 (25)	0.709 (17)	0.548 (4)			0.598 (6)		0.618 (10)
Validation											
MolProbity score	2.04	n/a	1.91	1.99	2.00	1.93	n/a	n/a	1.98	n/a	2.10
Clashscore	14.75		10.51	12.69	13.53	9.10			12.99		13.93
Poor rotamers (%)	0.00		0.00	0.03	0.00	0.00			0.00		0.00
Ramachandran plot											
Favored (%)	94.73	n/a	94.71	94.54	94.76	93.04	n/a	n/a	94.80	n/a	92.94
Allowed (%)	4.95		4.84	5.15	4.87	6.69			4.75		6.73
Disallowed (%)	0.31		0.45	0.31	0.37	0.28			0.45		0.33

Table 1 | Cryo-EM data collection, model refinement and validation statistics

Movie S1. The overall structure of an active MapSPARTA tetramer.

Movie S2. Structure of MapSPARTA dimer.

Movie S3. Structural basis for the activation of MapSPARTA complex.

Movie S4. Visualization of the enzymatic activity of Tir-domain NADase in MapSPARTA complex.